



## Experiment Report Form

**The double page inside this form is to be filled in by all users or groups of users who have had access to beam time for measurements at the ESRF.**

Once completed, the report should be submitted electronically to the User Office via the User Portal:

<https://www.esrf.fr/misapps/SMISWebClient/protected/welcome.do>

### ***Reports supporting requests for additional beam time***

Reports can be submitted independently of new proposals – it is necessary simply to indicate the number of the report(s) supporting a new proposal on the proposal form.

The Review Committees reserve the right to reject new proposals from groups who have not reported on the use of beam time allocated previously.

### ***Reports on experiments relating to long term projects***

Proposers awarded beam time for a long term project are required to submit an interim report at the end of each year, irrespective of the number of shifts of beam time they have used.

### ***Published papers***

All users must give proper credit to ESRF staff members and proper mention to ESRF facilities which were essential for the results described in any ensuing publication. Further, they are obliged to send to the Joint ESRF/ ILL library the complete reference and the abstract of all papers appearing in print, and resulting from the use of the ESRF.

Should you wish to make more general comments on the experiment, please note them on the User Evaluation Form, and send both the Report and the Evaluation Form to the User Office.

### **Deadlines for submission of Experimental Reports**

- 1st March for experiments carried out up until June of the previous year;
- 1st September for experiments carried out up until January of the same year.

### **Instructions for preparing your Report**

- fill in a separate form for each project or series of measurements.
- type your report, in English.
- include the reference number of the proposal to which the report refers.
- make sure that the text, tables and figures fit into the space available.
- if your work is published or is in press, you may prefer to paste in the abstract, and add full reference details. If the abstract is in a language other than English, please include an English translation.



	<b>Experiment title:</b> X-ray nanopatterning for magnonic logic gates	<b>Experiment number:</b> MA-3503
<b>Beamline:</b> ID 16B	<b>Date of experiment:</b> from: July 6 <sup>th</sup> 2017 to: July 11 <sup>th</sup> 2017	<b>Date of report:</b> September 9 <sup>th</sup> 2017
<b>Shifts:</b> 15	<b>Local contact(s):</b> Remi Tucoulou Tachoueres	<i>Received at ESRF:</i>

**Names and affiliations of applicants** (\* indicates experimentalists):

**F. J. Palomares\***, **J.M. González\***, **G. Martínez Criado\***, **U. Urdirroz\***, **E. Navarro\*** ICMN-CSIC, Dept. of nanostructures and surfaces, c/ Sor Juana Inés de la Cruz 3, 28049 Madrid, Spain; **M. Sánchez-Agudo\*** POEMMA-CEMDATIC, Dept. of physics electronics, ETSIST – UPM, c/ Nikola Tesla s/n, 28031 Madrid, Spain; **F. Cebollada\*** POEMMA-CEMDATIC, Dept. of physics electronics, ETSIT – UPM, Avenida Complutense 30, 28040 Madrid, Spain.

## Report

### Object:

Wave properties of guided magnons provide the foundations for the implementation of a new generation of process nanodevices whose major advantages are i) the fact that magnon propagation does not involve neither mass nor charge transport, thus allowing reduced energy consumption components, and ii) the possibility of designing logic gates based on simple interferometric principles. Despite these advantages, the viability of the magnonic process devices has not yet made fully clear due to open problems related to i) the implementation in the magnons guides of feasible wave properties modification functionalities (e.g.: controlled magnon phase shifters) and ii) the unavailability of reduced attenuation, guiding materials compatible with Si-nanofabrication. Our proposal focused on a magnon guides realisation candidate material: the amorphous  $F_{80}B_{20}$  alloy combining i) a magnon propagation length one order of magnitude longer than those corresponding to conventional Permalloy, and ii) the possibility of induction of different structural modifications (relaxation, atomic pairs diffusion induction and crystallization) resulting on variations of the effective magnetic anisotropy and, from that, of the characteristics of magnon propagation. Accordingly, our workplan included 1) the exploration of the synchrotron beam doses required to locally induce structural modifications in a- $Fe_{80}B_{20}$ , 2) the identification of the nature of those local modifications, and 3) the measurement of the magnon propagation parameters associated to the synchrotron beam induced local structural modifications. Regarding the third task, the particular measurement of the magnons phase shift associated to the irradiated regions (IRs) should provide the key ingredient to evaluate the feasibility of interferometric magnon logic gates.

### Samples:

The investigated a- $F_{80}B_{20}$  stripes (15 nm thick, 700  $\mu m$  long and having widths in the range from 2  $\mu m$  up to 16.4  $\mu m$ ) were prepared using UV lithography from continuous films grown onto single-crystal MgO substrates by using a pulsed laser ablation deposition device. Irradiation at ID16B was performed by using a beam with 56 nm x 56 nm spot size, and a maximum of the energy at  $E = 17.5$  keV with  $\Delta E/E = 10^{-2}$ . In order to identify the X-rays dosage required to structurally modify the a- $Fe_{80}B_{20}$ , fluxes from  $3,7 \times 10^{10}$  up to  $1.5 \times 10^{12}$  photons/s were used. The stripes were irradiated by using the single point, point-by-point line, point-by-point area, continuous line and continuous area scan modes. In the point-by-point irradiation cases the irradiation time was the parameter used to vary the dose in a range of photons per point going from  $3.7 \times 10^9$  up to  $3 \times 10^{13}$ . In some cases, several irradiation runs were carried out in the same stripe by illuminating areas from 50  $\mu m$  up to 350  $\mu m$  distant along the stripe axis. An in-house test, previous to the MA-3503 experiment, carried out by rapidly heating up to a temperature (450 °C) above that of the crystallization of the alloy 2 mm stripes lithographed on top of electrical contacts, revealed that the total resistance variation associated to the completion of the crystallization corresponded to a 12% reduction. Since the regions to be structurally modified during the irradiation should have maximum widths along the stripe long directions of a few hundreds of nm ( $10^{-4}$  of the total stripe length), the expected maximum resistance change per strip was below our experimental resolution. The negative result of this test lead us to not carry out any resistance in-operando measurements.

### Results:

Previously to the MA-3503 experiment, magneto-optic Kerr effect (MOKE) measurements of the hysteretic behaviour of the stripes were carried out. These measurements evidenced the homogeneity of the samples since local loops measured along the stripes long direction showed coercivities independent of the measuring position. Also, it was possible to identify an increase of the coercive force associated to the stripes width reduction from 12.2 Oe measured in the 16,4  $\mu m$  samples up to 17.2 Oe measured in the 4  $\mu m$  samples. This result confirmed the occurrence in our stripes of a wall propagation/pinning mediated magnetization reversal process, in agreement with previous Kerr microscopy direct observation of the occurrence of that process in a- $F_{80}B_{20}$  continuous films [1].

The samples were in-operando examined by optical microscopy and, after irradiation, in-situ observed by SEM, which showed that a dose of  $3 \times 10^{13}$  photons per point (point-by-point line scan,  $1.5 \times 10^{12}$  photons/s during 20 s per point) resulted on the distinguishable evolution of the stripe morphology during the irradiation and on the presence, identified once irradiation was completed, of stripe-wide areas, hundreds of  $\mu\text{m}$  long, exhibiting a morphology indicating the occurrence of extended, uncorrelated to the irradiation localization, melting/solidification processes. The MOKE hysteresis loop measured in that stripe revealed a coercivity of 7 Oe, ca. 50% below the value measured prior to irradiation. None of the other irradiation runs, carried out using lower doses, resulted in SEM detectable morphology changes.

MOKE measurements were carried out ex-situ in all the irradiated samples. The measurements were collected by displacing a  $15 \mu\text{m}$  wide spot along the length of the stripes in order to obtain information about the local hysteresis of both the irradiated and non-irradiated areas. Our results (see Figure 1) revealed that, for a flux of  $2.21 \times 10^{11}$  photons/s and a total dose per point of  $2 \times 10^{11}$  photons, the measurement of the local coercive force at different irradiated regions (IR) in continuous area scans carried out at points separated by  $100 \mu\text{m}$  in the same stripe, depended on the nominal transverse dimensions of those IR. That dependence, corresponding to a total coercivity increase of 20% can be understood by recalling that the magnetization reversal mechanisms of our samples corresponds to the wall propagation/pinning type and the fact that, from our previous measurements of the a- $\text{F}_{80}\text{B}_{20}$  magnetic anisotropy [1], the width of a Bloch wall is approximately 400 nm.

A propagating wall gets pinned along its path (the stripe axis in our case) when it finds a pinning centre at which the wall lowers its energy. The depinning field (the local coercivity) measures the wall energy decrease. That decrease corresponds in the 60 nm and 120 nm cases, to IR having a nominal width lower than that of the wall, in that of the 360 nm region to a width similar to that of the wall and a crossover occurs for the 720 nm and 1440 nm IR having widths larger than the wall width. For the IR with widths smaller than the pinned wall width the energy decrease/local coercivity corresponds to a fraction of the wall width and, consistently, it increases with the increase of the IR width up to a value of the order of that of the width of the wall. When the crossover to IR wider than the wall occurs the depinning field is given by the difference in wall energy inside and outside the IR and it is therefore independent of the IR width.

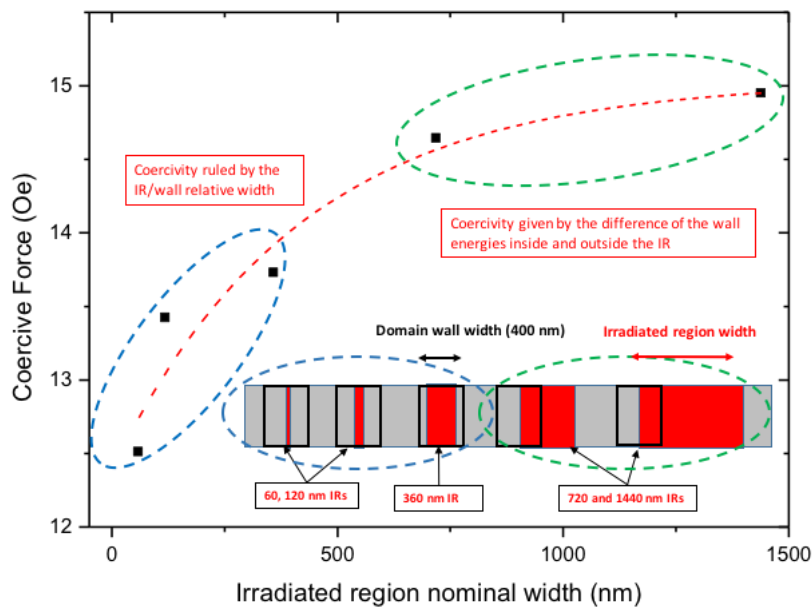


Figure 1. Local coercivity measured by MOKE in IR having different nominal widths. The inset illustrates the relationship of the IR/wall relative dimensions with the local coercivity

### Conclusions:

Our conclusions partly cover objectives 1) (irradiation dosage identification) and 2) (nature of the changes induced in the material) of our proposal. Objective 3) was not dealt with due to the incompleteness of the previous ones.

The event in our samples of a propagation/pinning reversal mechanism allows to use the dependence of the local coercivity on the IR nominal dimensions and the wall width as an indicator of the occurrence of irradiation induced magnetic properties modifications and an IR effective dimensions measure, respectively. From our results, we conclude that:

- For doses below  $3 \times 10^{13}$  photons the IR can be correlated to local coercive force variations and therefore to local magnetic properties modifications. The coercivity of IR produced using different fluxes but having the same transverse dimensions are indistinguishable.
- The crossover in the IR width dependence of the local coercivity taking place at a nominal IR width similar to the wall width indicates that the effective scale of the IR transverse dimensions is comparable to the nominal one.
- The magnitude of the coercivity increase associated to irradiation suggest the induction during this process of moderate anisotropy reductions and, consequently, of structural relaxation.

[1] U. Urdiruz, F.J. Palomares, F. Cebollada, J.M. Alameda, J.M. González. Submitted to Journal of Magnetism and Magnetic Materials